Volume 16 Number 14 1988 Nucleic Acids Research

The fidelity of base selection by the polymerase subunit of DNA polymerase III holoenzyme

David L.Sloane, Myron F.Goodman[1] and Harrison Echols

Department of Molecular Biology, University of California-Berkeley, Berkeley, CA 94720 and
[1]Department of Biological Sciences, University of Southern California, Los Angeles, CA 90089, USA

Received March 2, 1988

ABSTRACT

In common with other DNA polymerases, DNA polymerase III holoenzyme of *E. coli* selects the biologically correct base pair with remarkable accuracy. DNA polymerase III is particularly useful for mechanistic studies because the polymerase and editing activities reside on separate subunits. To investigate the biochemical mechanism for base insertion fidelity, we have used a gel electrophoresis assay to measure kinetic parameters for the incorporation of correct and incorrect nucleotides by the polymerase (α) subunit of DNA polymerase III. As judged by this assay, base selection contributes a factor of roughly 10^4-10^5 to the overall fidelity of genome duplication. The accuracy of base selection is determined mainly by the differential K_M of the enzyme for correct vs. incorrect deoxynucleoside triphosphate. The misinsertion of G opposite template A is relatively efficient, comparable to that found for G opposite T. Based on a variety of other work, the G:A pair may require a special correction mechanism, possibly because of a syn-anti pairing approximating Watson-Crick geometry. We suggest that precise recognition of the equivalent geometry of the Watson-Crick base pairs may be the most critical feature for base selection.

INTRODUCTION

Genomic duplication is carried out with remarkable fidelity. Error frequencies in the duplication of the *Escherichia coli* genome are 10^{-9} to 10^{-10} per base replicated (1). This high fidelity is achieved by a three-step process: 1) the correct selection of the complementary deoxynucleoside triphosphate substrate during 5' → 3' incorporation (base selection); 2) exonucleolytic 3' → 5' editing of a noncomplementary deoxynucleoside monophosphate misinserted at the end of the growing chain; 3) post-replicative mismatch repair. The summation of the estimated contributions of each of these three steps results in the observed accuracy (2-4).

DNA polymerase III holoenzyme (pol III) is responsible for the majority of chromosomal replication in *E. coli* and is therefore probably the major determinant of the fidelity of genome duplication (2, 3). We have initiated experiments designed to investigate the contribution and mechanism of base selection and editing in the fidelity of replication by pol III. The pol III holoenzyme is composed of 10 different subunits: α, ε, θ, τ, γ, δ, δ', χ, ψ, and β (5). The subunits α, ε and θ compose the smallest subassembly of pol III prepared from the holoenzyme, called pol III core (6). The α subunit, the *dnaE* gene product (7), has the 5' → 3' polymerase activity (8). The ε subunit, the *dnaQ* gene product (9), carries the 3' → 5' exonuclease activity (10). Therefore, in pol III holoenzyme the base selection and editing activities reside on two distinct subunits, α and

ε, respectively. The polymerase subunit can be prepared separately in active form (5, 8), and so base selection can be studied in the absence of editing.

A polymerase has two general mechanisms that might distinguish between correct and incorrect base pairs: differential binding in the active site, and differential catalysis of phosphodiester bonds dependent on prior binding of the correct pair. Some information about the relative importance of these mechanisms can be derived from the kinetic parameters of nucleotide incorporation, K_M and V_{max}. The ratio V_{max}/K_M measures the efficiency of nucleotide insertion and thus determines the specificity for competing substrates; the misinsertion frequency of the polymerase is given by the ratio of V_{max}/K_M for incorrect vs. correct nucleotides (11, 12). If we assume that differences in K_M reflect mainly differences in the K_D for dNTP, the differential binding model predicts that the misinsertion frequency will depend on the relative K_M for incorrect vs. correct nucleotides. An analysis of this "K_M discrimination model" based on experiments with T4 polymerase and eukaryotic polymerase α have been presented previously (12-15). For DNA polymerase I, even though the detailed reaction pathway is complex, the steady state K_M (~1-2 μM) is close to the estimated K_D (~5 μM) (16, 17). In a mechanism involving selective phosphodiester bond formation, the correct base pair is selected after the binding step (18, 19). To the extent that V_{max} for nucleotide incorporation is determined by phosphodiester bond formation, this mechanism would result in "V_{max} discrimination." [However, for DNA polymerase I dissociation from DNA is rate-limiting for nonprocessive DNA synthesis (17).]

In the work reported here, we have used a gel electrophoresis assay to estimate the K_M and relative V_{max} for incorporation of correct and incorrect nucleotides by the polymerase (α) subunit of pol III. Our results indicate that the accuracy of base selection is determined mainly by the differential K_M of the enzyme for correct vs. incorrect deoxynucleoside triphosphate. From our results and other work, we suggest that precise recognition of the equivalent geometry of the Watson-Crick base pairs is likely to be the most critical feature for base selection.

MATERIALS AND METHODS

Materials

Purified α subunit of DNA polymerase III was a generous gift of Hisaji Maki and Arthur Kornberg, Stanford University. The 16-base deoxynucleotide primer, the 30-base deoxynucleotide template and the M13 primers were machine synthesized using standard phosphoramidite chemistry. The dNTP substrates and FPLC pure T4 polynucleotide kinase were purchased from Pharmacia. Radioactive [γ-^{32}P] ATP (>5000 Ci/mmole, 10 mCi/ml) was purchased from Amersham. Single-stranded wild-type M13 DNA was prepared by published procedures (20). The sequence of the DNA used for misinsertion target 1 is shown below:

```
5' - G C G C C G C C A A A A C G T C - 3'
     | | | | | | | | | | | | | | | |
3' - C G C G G C G G T T T T G C A G G G A T C C G A T T G C A G - 5'
```

Primer Labeling

The 5' termini of DNA primers were labeled with ^{32}P in a 50 µl reaction mixture containing 70 mM Tris-HCl (pH 8.0), 10 mM $MgCl_2$, 5 mM DDT, 0.8 µM [γ-^{32}P] ATP, 4 µM primer oligonucleotide and 20 units polynucleotide kinase. The solution was incubated at 37°C for 1.5 hours and the reaction terminated by the addition of NaAcetate to 0.3 M and 150 µl 100% ethanol. The DNA was precipitated, washed once with 70% ethanol, dried in a Savant Speed-Vac concentrator and resuspended in 20 µl glass distilled H_2O.

Primer-Template Annealing

For the oligonucleotide template, the primer was annealed to the template in a reaction mixture containing 10 mM Tris-HCl (pH 8.0), 200 mM NaCl, 3.8 µM primer, and 19 µM template (5:1 template:primer ratio). This mixture was heated to 70°C for ten minutes and allowed to slowly cool to room temperature (2-3 hours). The mixture was then passed over a 1 ml Sephadex G-50 column to remove any unincorporated [γ-^{32}P] ATP and salt. DNA peak fractions were measured by Cerenkov counting, pooled and ethanol precipitated. The DNA pellet was then dried and resuspended in 150 µl TE (10 mM Tris-HCl (pH 8.0), 1 mM EDTA). M13 primers and templates were prepared in a similar way as above, except the annealing was at a primer:template ratio of 1.5:1, and the G-50 column and ethanol precipitation steps were omitted (12).

DNA Polymerase Reactions

For the oligonucleotide template, reaction mixtures (25 µl) contained 33 mM MOPS (pH 7.0), 80 µg/ml BSA, 10 mM $MgCl_2$, 8.5 mM DTT, 4.8% polyethylene glycol, 40 nM primed DNA template and various concentrations of dNTPs. The mixture was incubated at 25°C for either 2 minutes (correct insertion) or 10 minutes (misinsertion). Reactions were quenched by the addition of 78 µl 97% ethanol/97 mM NaAcetate, and the DNA precipitated. The DNA pellets were then dried and resuspended in 3 µl 99% formamide. Time course experiments were done to determine a suitable reaction time for kinetic studies. The reaction conditions for these experiments were the same as above except the incubation time varied between 1 and 20 minutes. For the M13 template, a slightly modified protocol was used (12); the volumes of the reaction mixtures were 6 µl, and the reactions were quenched by adding 12 µl of 96% formamide/32 mM EDTA.

Gel Electrophoresis and Autoradiography

The DNA samples in formamide were heated to 100°C for five minutes, cooled on ice, loaded onto a 15% polyacrylamide gel containing 8 M urea, and then electrophoresed at 1800 volts until a bromphenol blue dye had just run off the gel. For autoradiography, the gels were overlayed with Kodak XRP-1 film.

Densitometry

The autoradiographs were scanned on a Hoeffer GS300 densitometer at 6.5 cm/minute. Band areas were determined with a Hoeffer GS350 data system integrating peak areas. The densitometer was calibrated against a Kodak photographic step tablet and gave a linear response up to an absorbance equal to 2.0. Varying quantities of ^{32}P-labeled primer were run on gels and autoradiographs

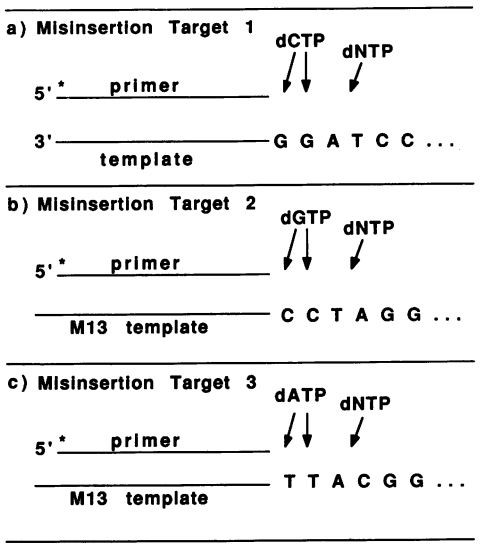

Figure 1. Schematic representations of the polymerase reactions used to derive kinetic parameters for insertion of correct or incorrect nucleotides (see Methods). All primers were machine synthesized and labeled at the 5'-end with ^{32}P. In each case, a substrate dNTP was added at a saturating concentration (25 μM) to allow extensions opposite the first two template bases at maximum velocity. Various concentrations of substrate dNTP were added to allow kinetic measurement of insertion at the target site, the third template base. a) For misinsertion target 1, the template was a synthetic 30-base oligonucleotide, primed with a synthetic 16-base primer. The target site was an A. b) For misinsertion target 2, the template was M13 single-stranded DNA primed at nucleotides 2225-2248 with a 23-base primer. The target site was a T. c) For misinsertion target 3, the template was M13 single-stranded DNA, primed at nucleotides 1269-1285 with a 17-base primer. The target site was an A.

taken to determine the linear range of film response. These autoradiographs were then scanned. The band intensities in arbitrary units were found to increase linearly with counts per minute up to 12,000 units, and the film has a threshold value of 150 units. Consequently, for kinetic experiments, the exposure times were selected so that the highest band intensity was under 10,000 units, and a value of 150 was added to each measured intensity.

RESULTS

The experiments have been designed to measure the kinetic parameters for insertion of correct or incorrect deoxynucleotide opposite a single target base on a template. A schematic representation of the reactions is presented in Figure 1. For misinsertion target 1, the target A site is located 3 bases downstream from the primer 3' terminus (Fig. 1a). Before reaching this site, the polymerase must correctly insert C nucleotides opposite the first two template G residues. The 5'-terminus of the primer is labeled with ^{32}P so that extensions of one, two, and three nucleotides appear as discrete bands on an autoradiograph of the polyacrylamide gel. There are never more than two deoxy-

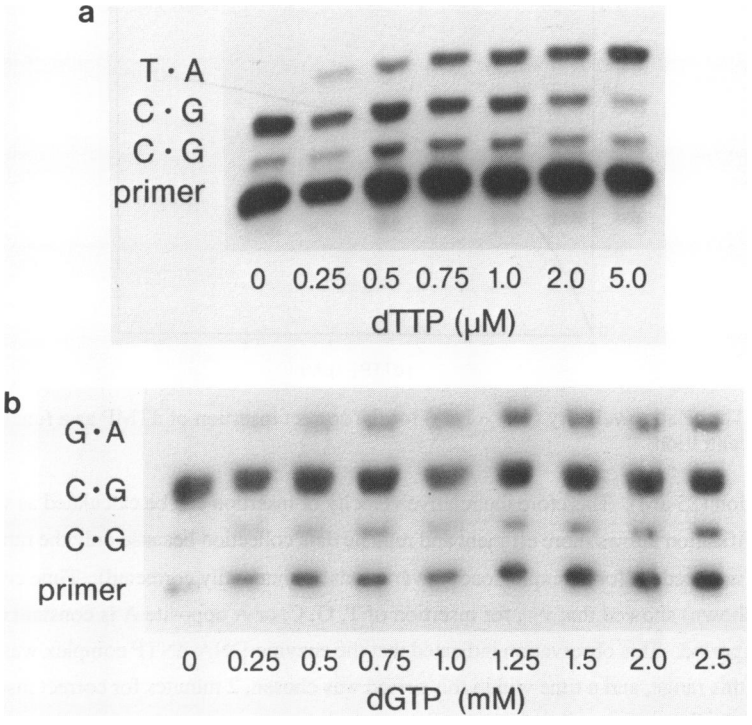

Figure 2. Gel autoradiograms showing the extension of the primer by the α subunit of DNA polymerase III as a function of added dNTP substrate. The substrate DNA for this extension is in Figure 1 (a). DNA polymerase reactions were done with varying concentrations of (a) dTTP or (b) dGTP. In each case, there is 25 μM dCTP to allow insertions at sites 1 and 2 to proceed at maximum velocities.

nucleotide triphosphates in the reaction mixture so longer extensions are not possible.

Kinetic analysis of primer extension by a polymerase lacking a 3' → 5' exonuclease has shown that the velocity of chain extension from template site 2 to site 3, $v_{2\text{-}3}$, is expected to obey the Michaelis-Menten equation (12):

$$v_{2\text{-}3} = V_{max}[S] / K_M + [S]$$

Therefore, at steady state, we can determine the V_{max} and K_M of the reaction by varying the concentration of the dNTP to be inserted at site 3.

The experimental data are the integrated band intensities, I_2 and I_3, derived from densitometric scanning of autoradiographs of the gels (Fig. 2). The velocity of chain extension can be expressed as (12):

$$v_{2\text{-}3} = \frac{I_2 + I_3}{t} \cdot \frac{I_3}{I_2}$$

At a constant time point (t) the factor $(I_2 + I_3/t)$ is constant when dCTP is present at a saturating

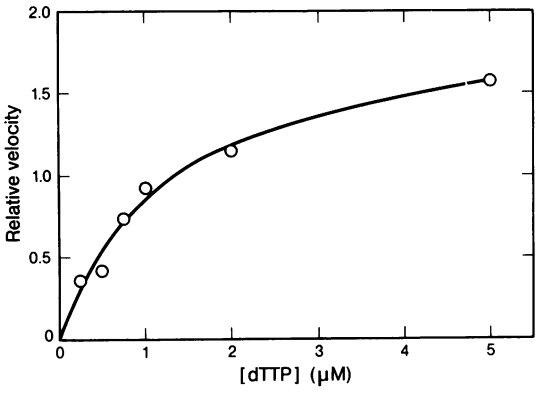

Figure 3. The relative velocity ($v_{2-3} = I_3/I_2$) for the correct insertion of dTMP as a function of dTTP concentration.

concentration (25 μM). Therefore the relative velocity of insertion can be calculated as $v = I_3/I_2$. This simplification allows more efficient and reliable data collection because only the ratio of band intensities are needed (for example, loading variations are internally corrected). Time course studies (not shown) showed that v_{2-3} for insertion of T, G, C, or A opposite A is constant over a 5 to 10 minute period. This observation indicated that the enzyme-DNA-dNTP complex was in steady state over this range, and a time within this period was chosen, 2 minutes for correct insertion and 10 minutes for incorrect.

Misinsertion Target 1

At misinsertion target 1 (Fig. 1a), the α polymerase subunit was incubated with dCTP for the first two additions to the primer and with either dTTP, dGTP, or dATP to determine the kinetic parameters for correct or incorrect insertion opposite template A. The autoradiographic data for dTTP and dGTP are shown in Fig. 2. A plot of v_{2-3} *vs.* dNTP for dTTP or dGTP showed typical saturation kinetics (Fig. 3 and Fig. 4). The apparent K_M and relative V_{max} values were determined from a linear least squares fit of a Hanes-Woolf plot ([S]/v *vs.* [S]) of each insertion opposite A (Table 1).

The apparent K_M for misinsertion of G opposite A (400 μM) is 400 times greater than for the correct T opposite A (1 μM). The relative V_{max} is five-fold lower. Therefore, the misinsertion of G opposite A is discriminated against mainly by K_M. The ratio of V_{max}/K_M, which is the initial slope of the v *vs.* [dNTP] plot, measures the efficiency of nucleotide insertion by polymerase (11). The ratio of incorrect *vs.* correct insertion efficiencies is the misinsertion frequency of the polymerase.

The G:A mismatch was the easiest for the α subunit to make at this target site. The insertion efficiency for C:A was 7-fold less and the efficiency for A:A was at least 40-fold less than G:A. For the insertion of C opposite A, the K_M is 10^3-fold higher than for the correct insertion, and the

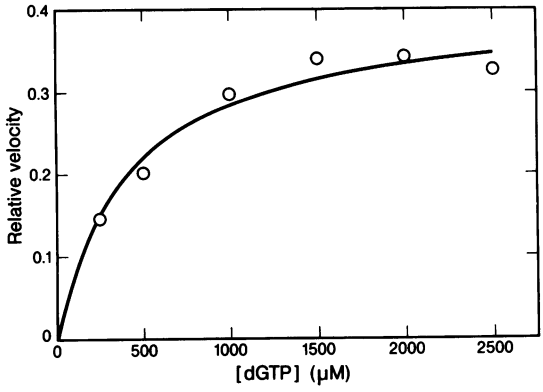

Figure 4. The relative velocity ($v_{2-3} = I_3/I_2$) for the incorrect insertion of dGMP as a function of dGTP concentration.

V_{max} is ten-fold less. The insertion of A opposite A was barely detectable, and so quantitative data could not be obtained; the K_M was clearly very high.

Misinsertion Target 2

We have also analyzed misinsertions opposite a template T. A 23 base primer was used with single-stranded M13 DNA as template (Fig. 1b). Data for the insertion of A or G opposite T are presented in Table 2. The insertion of T opposite T or C opposite T was not detected under the conditions studied so far and so must be extremely inefficient. The misinsertion of G opposite T occurs with comparable efficiency to G opposite A. The K_M value for the misinsertion of G oppo-

Kinetic Parameters at Misinsertion Target 1

dNTP	K_M (μM)	relative V_{max}	V_{max}/K_M (M^{-1})	Misinsertion Frequency	n
dTTP	1.0 ± 0.2	2.0 ± 0.2	2.1×10^6	1	4
dGTP	400 ± 2	0.43 ± 0.02	1.1×10^3	5.2×10^{-4}	3
dCTP	1160 ± 130	0.17 ± 0.02	1.5×10^2	7.1×10^{-5}	3
dATP	~1500	~0.04	$\sim 2.7 \times 10^1$	$\sim 1.3 \times 10^{-5}$	2

Table I. Relative V_{max} and apparent K_M values for the α subunit at misinsertion target 1 (insertion opposite a template A). The relative velocity of insertion was measured as the ratio of band intensities, $v_{2-3} = I_3/I_2$, as determined by gel electrophoresis and autoradiography. A Hanes-Woolf plot of [dNTP]/v *vs.* [dNTP] was fitted linearly by least-squares to determine the intercept (K_M/V_{max}) and slope ($1/V_{max}$). The mean K_M and V_{max} values are shown ± standard error found in repeated experiments (n) with each substrate.

Kinetic Parameters at Misinsertion Target 2

dNTP	K_M (μM)	relative V_{max}	V_{max}/K_M (M^{-1})	Misinsertion Frequency	n
dATP	4.0 ± 0.3	4.0 ± 0.4	1×10^6	1	2
dGTP	680 ± 57	0.15 ± 0.02	2.2×10^2	2.2×10^{-4}	2

Table II. Relative V_{max} and apparent K_M values for the α subunit at misinsertion target 2 (insertion opposite a template T). The apparent K_M and relative V_{max} values were determined in the same way as in Table 1. Values shown are the averages of duplicate experiments ± standard error. The fit to a Hanes-Woolf plot of each experiment gave a correlation coefficient of greater than 0.98. The insertion of T or C opposite template T was undetectable.

site T is 170 times larger than for A opposite T and the V_{max} value is 27-fold less. Thus the misinsertion of G opposite T is discriminated against mainly by K_M.

Misinsertion Target 3

We have obtained limited data with a third misinsertion target, which largely corroborates that obtained with the first. These results are presented in Table 3. Misinsertions opposite a template A were studied with single-stranded M13 DNA as template and a 17-base primer that provided a different sequence environment from the first A target site (Fig. 1c). The misinsertion frequency for the C:A pair was about the same as for Table 1. The A:A misinsertion was not detectable; however, it was only barely discernable previously. The misinsertion frequency for G:A was some 5-fold lower than for the site of Table 1. However, in this case the analysis is complicated because G is the correct base for the template C that follows the target A site (Fig. 1c); therefore, the kinetic data are based on measurement of the G:C band at the fourth template site because the G:A band at the third site is not detectable at high concentrations of dGTP. Since the primer for the data band

Kinetic Parameters at Misinsertion Target 3

dNTP	K_M (μM)	relative V_{max}	V_{max}/K_M (M^{-1})	Misinsertion Frequency	n
dTTP	4.1 ± 1.0	1.6 ± 0.07	3.9×10^5	1	2
dGTP	3050 ± 35	0.14 ± 0.01	4.6×10^1	1.2×10^{-4}	2
dCTP	2000 ± 140	0.06 ± 0.01	3.0×10^1	7.7×10^{-4}	2

Table III. Relative V_{max} and apparent K_M values for the α subunit at misinsertion target 3 (insertion opposite a template A). The apparent K_M and relative V_{max} values were determined in the same way as in Table 1. Values shown are the averages of duplicate experiments ± standard error. The fit to a Hanes-Woolf plot of each experiment gave a correlation coefficient of greater than 0.98. The insertion of A opposite A at this sequence was undetectable.

carries a G:A mispair, the incorporation of the next correct base might be hampered, and thereby the misinsertion frequency for G:A underestimated. Additional experiments that start with mispaired primers should clarify this point. In any case, the misinsertion at the G:A mispair does occur with substantial efficiency, as for the first template-primer system.

DISCUSSION

Possible Geometric Mechanism for K_M Discrimination

We have used a gel electrophoresis assay to measure kinetic parameters for the incorporation of correct and incorrect nucleotides by the polymerase subunit of pol III holoenzyme. We estimate that the capacity of the enzyme to choose a correct over an incorrect base pair is in the range of 10^4-10^5. For some pairs, the discrimination may be considerably greater because we have not been able to detect the misinsertion. For each example for which we have quantitative data, the discrimination against misinsertion is mainly through the differential K_M of the enzyme for correct vs. incorrect triphosphate. If these differences in K_M reflect mainly differences in the K_D for correct or incorrect dNTP, highly preferential binding of the correct substrate is likely to be the primary mechanism for accurate base selection. The enzyme-DNA-dNTP complex is more stable when the dNTP is complementary to the template base than when it is not. A similar conclusion has been derived for T4 DNA polymerase and eukaryotic polymerase α (12-15).

The molecular mechanism for the impressive K_M discrimination is of course not revealed by the kinetic data. If we adopt the binding model, there is clearly a large amplification in the differential binding energy beyond that provided by differential capacity to form hydrogen bonds. One mechanism that can provide for this amplification is a geometric recognition mechanism in which the active site of the polymerase is designed to accept the geometrically identical Watson-Crick base pairs, A:T and G:C, and reject those base-pairs deviating from this geometry (a "micrometer" enzyme) (3, 21). The relatively efficient misinsertion at G:A and G:T pairs lends some support to this model. The G:T pair is the classical "wobble" pair that can form two hydrogen bonds; this pair has nearly canonical C1'-C1' distances, but a substantial angular wobble (22). Based on X-ray crystallography of mismatched oligonucleotides, a G(anti):A(syn) pair has been identified that approximates even more closely the Watson-Crick geometry with somewhat less of an angular wobble than G:T (21). [A G(anti): A(anti) pair has also been suggested from NMR analysis (23, 24).] Thus the geometric discrimination mechanism is consistent with the currently available (though limited) data on base-pair geometry and misinsertion frequencies by the polymerase subunit of pol III holoenzyme. Geometric discrimination might also operate at other stages of the polymerase reaction than the dNTP binding step, and might contribute to the V_{max} effects that we observe through less effective phosphodiester bond formation due to the angular wobble of the mispair.

Transversion Correction: Special Problem of a G:A Pair

Our observation of relatively efficient misinsertion of G opposite A poses some interesting problems for the subsequent correction systems, exonucleolytic editing and mismatch repair. A

generalization of the geometric argument would suggest that a G:A pair might be poorly edited and subject to inefficient mismatch correction because of its close approximation to the geometry of the A:T and G:C pairs. Data on mismatch repair *in vivo* and *in vitro* indicate generally poor correction for G:A (25, 26). Indirect data on editing *in vitro* also indicate inefficient correction of G:A errors (27). These considerations suggest that there may be special mechanisms for the avoidance of transversion mutations derived from G:A mispairs. If the Mut mismatch correction system is removed *in vivo* by mutation, transversion mutations are very rare (1/25 of transitions) (28, 29). This observation raises explicitly the possibility of a special G:A correction system. The existence of such a system can be inferred from mutator mutations that specifically increase the frequency of transversion errors deriving from G:A pairs. Mutations in the *mut*T gene increase A:T → C:G mutations by 10^2-10^4 (30). Mutations in the *mut*Y gene increase G:C → T:A mutations by about 10^2 (31). Recent work has indicated that *mut*T acts during DNA replication in crude extracts to avoid G:A mispairs (32). Thus, a second type of editing function might be associated with pol III holoenzyme, avoiding misinsertions derived from G:A mispairs. Alternatively, a special mismatch correction system operative in the extract might be involved. Interestingly, recent data on mismatch repair *in vitro* suggest that a repair mechanism other than the Mut pathway converts G:A to G:C (26). Thus, the G:A mispair appears to pose special problems for error avoidance, which are solved by special correction mechanisms. The relative contribution of replicative and post-replicative systems remains to be elucidated.

ACKNOWLEDGEMENTS

This work was supported by grants from the National Institutes of Health (CA 46155, GM 21422, GM 33863). We thank Arthur Kornberg and Hisaji Maki for their gift of the α subunit of Pol III holoenzyme. We also thank Michael Boosalis and Lynn Mendelmans for technical advice and helpful discussions, and Murray Deutscher and Judith Klinman for valuable comments on the manuscript. One of us (H.E.) gives special birthday thanks to Arthur Kornberg for his hospitality during a sabbatical leave that provided a "license to do biochemistry."

REFERENCES

1. Drake, J.W. (1969) *Nature (London)* **221**, 1132.
2. Kornberg, A. (1980) *DNA Replication*, Freeman, San Francisco.
3. Echols, H. (1982) *Biochimie* **64**, 571-575.
4. Loeb, L.A. and Kunkel, T.A. (1982) *Ann. Rev. Biochem.* **51**, 429-458.
5. Kornberg, A. (1988) *J. Biol. Chem.* **263**, 1-4.
6. McHenry, C.S. and Crow, W. (1979) *J. Biol. Chem.* **254**, 1748-1753.
7. Welch, M. and McHenry, C.S. (1982) *J. Bacteriol.* **152**, 351-356.
8. Maki, H. and Kornberg, A. (1985) *J. Biol. Chem.* **260**, 12987-12992.
9. Scheuermann, R.H., Tam, S., Burgers, P.M.J., Lu, C. and Echols, H. (1983) *Proc. Natl. Acad. Sci. USA* **80**, 7085-7089.
10. Scheuermann, R.H. and Echols, H. (1984) *Proc. Natl. Acad. Sci. USA* **81**, 7747-7751.
11. Fersht, A.R. (1985) *Enzyme Structure and Mechanism*, W.H. Freeman and Company, New York.
12. Boosalis, M.S., Petruska, J. and Goodman, M.F. (1987) *J. Biol. Chem.* **262**, 14689-14696.
13. Galas, D.J. and Branscomb, E.W. (1978) *J. Mol. Biol.* **124**, 653-687.

14. Watanabe, S.M. and Goodman, M.F. (1982) *Proc. Natl. Acad. Sci. USA* **79**, 6429-6433.
15. Goodman, M.F. and Branscomb, E.W. (1986) In Kirkwood, T.B.L., Rosenberger, R.F. and Galas, D.J. (eds.), *Accuracy in Molecular Processes,* Chapman and Hall, London, pp. 191-232.
16. McClure, W.R. and Jovin, T.M. (1975) *J. Biol. Chem.* **250**, 4073-4080.
17. Kuchta, R.D., Mizrahi, V., Benkovic, P.A., Johnson, K.A. and Benkovic, S.J. (1987) *Biochemistry* **26**, 8410-8417.
18. Koch, A.L. and Miller, C. (1965) *J. Theoret. Biol.* **8**, 17-80.
19. Speyer, J.F., Karam, J.D. and Lenny, A.B. (1966) *Cold Spring Harbor Symp. Quant. Biol.* **31**, 693-697.
20. Messing, J. (1983) *Meth. Enzymol.* **101**, 20-78.
21. Brown, T., Hunter, W.N., Kneale, G. and Kennard, O. (1986) *Proc. Natl. Acad. Sci. USA* **83**, 2402-2406.
22. Brown, T., Kennard, O., Kneale, G. and Rabinovich, D. (1985) *Nature* **315**, 604-606.
23. Kan, L.-S., Chandrasegaran, S., Pulford, S.M. and Miller, P.S. (1983) *Proc. Natl. Acad. Sci. USA* **80**, 4263-4265.
24. Patel, D.J., Kozlowski, S.A., Ikuta, S. and Itakura, K. (1984) *Biochemistry* **23**, 3207-3217.
25. Modrich, P. (1987) *Ann. Rev. Biochem.* **56**, 435-466.
26. Su, S.-S., Lahue, R.S., Au, K.G. and Modrich, P. (1988) *J. Biol. Chem.*, in press.
27. Fersht, A.R., Shi, J.-P. and Tsui, W.C. (1983) *J. Mol. Biol.* **165**, 655-669.
28. Leong, P.-M., Hsia, H.C. and Miller, J.H. (1986) *J. Bacteriol.* **168**, 412-416.
29. Schaaper, R.M. and Dunn, R.L. (1987) *Proc. Natl. Acad. Sci USA* **84**, 6220-6224.
30. Cox, E.C. (1973) *Genetics* **73** (suppl.), 67-80.
31. Nghiem, Y., Cabrera, M., Cupples, C.G. and Miller, J.H. (1988) *Proc. Natl. Acad. Sci. USA* **85**, in press.
32. Schaaper, R.M. and Dunn, R.L. (1987) *J. Biol. Chem.* **262**, 16267-16270.